

Unravelling the Interactions between Surface-Active Ionic Liquids and Triblock-Copolymers for the Design of Thermal Responsive Systems

German Perez-Sanchez, Filipa A. Vicente, Nicolas Schaeffer, Inês S. Cardoso, Sonia P.M. Ventura, Miguel Jorge, and Joao A.P. Coutinho

J. Phys. Chem. B, **Just Accepted Manuscript** • DOI: 10.1021/acs.jpcc.0c02992 • Publication Date (Web): 20 Jul 2020

Downloaded from pubs.acs.org on July 25, 2020

Just Accepted

“Just Accepted” manuscripts have been peer-reviewed and accepted for publication. They are posted online prior to technical editing, formatting for publication and author proofing. The American Chemical Society provides “Just Accepted” as a service to the research community to expedite the dissemination of scientific material as soon as possible after acceptance. “Just Accepted” manuscripts appear in full in PDF format accompanied by an HTML abstract. “Just Accepted” manuscripts have been fully peer reviewed, but should not be considered the official version of record. They are citable by the Digital Object Identifier (DOI®). “Just Accepted” is an optional service offered to authors. Therefore, the “Just Accepted” Web site may not include all articles that will be published in the journal. After a manuscript is technically edited and formatted, it will be removed from the “Just Accepted” Web site and published as an ASAP article. Note that technical editing may introduce minor changes to the manuscript text and/or graphics which could affect content, and all legal disclaimers and ethical guidelines that apply to the journal pertain. ACS cannot be held responsible for errors or consequences arising from the use of information contained in these “Just Accepted” manuscripts.

Unravelling the Interactions between Surface-Active Ionic Liquids and Triblock-Copolymers for the Design of Thermal Responsive Systems

Germán Pérez-Sánchez^{1,†,}, Filipa A. Vicente^{1,†}, Nicolas Schaeffer¹, Inês S. Cardoso¹, Sónia P. M. Ventura¹, Miguel Jorge^{2,*} and João A. P. Coutinho¹*

¹CICECO, Departamento de Química, Universidade de Aveiro, 3810-193 Aveiro, Portugal

²Department of Chemical and Process Engineering, University of Strathclyde, 75 Montrose Street, Glasgow G1 1XJ, United Kingdom

*Corresponding authors

[†]Both authors contributed equally

Campus Universitário de Santiago, Universidade de Aveiro, Aveiro, Portugal

Tel: +351-234-370200; Fax: +351-234-370084; E-mail addresses: german@ua.pt,
miguel.jorge@strath.ac.uk

1 ABSTRACT

2 The tuneable properties of surface-active ionic liquids (SAIL) and Pluronics are dramatically
3 magnified by combining them in aqueous solutions. The thermo-controlled character of both,
4 essential in the extraction of valuable compounds, can be fine-tuned by properly selecting the
5 Pluronic and SAIL nature. However, further understanding of the nanoscale interactions directing
6 the aggregation in these complex mixtures is needed to effectively design and control these
7 systems. In this work, a simple and transferable coarse-grained model for molecular dynamics
8 simulations, based on the MARTINI force field, is presented to study the impact of SAILS in
9 Pluronics aggregation in aqueous solutions. The diverse amphiphilic characteristics and micelle
10 morphologies were exemplified by selecting four archetypical non-ionic Pluronics; two normal,
11 L-31 and L-35 and, two reverse, 10R5 and 31R1. The impact of the alkyl-chain length and the
12 headgroup nature were evaluated with the imidazolium $[C_{10}mim]Cl$, $[C_{14}mim]Cl$ and
13 phosphonium-based $[P_{4,4,4,14}]Cl$ SAILS. Cloud point temperature (CPT) measurements at different
14 Pluronic concentrations with 0.3 %wt of SAIL in aqueous solution emphasised the distinct impact
15 of SAIL nature on the thermo-response behaviour.

16 The main effect of SAIL addition to non-ionic Pluronics aqueous solutions is the formation of
17 Pluronic/SAIL hybrid micelles, where the presence of SAIL molecules introduces a charged
18 character to the micelle surface. Thus, additional energy is necessary to induce micelle
19 aggregation, leading to the observed increase in the experimental CPT curves. The SAIL showed
20 a relatively weak impact in Pluronic micelles with relatively high PPG hydrophobic content,
21 whereas this effect was more evident when the Pluronic hydrophobic/hydrophilic strength is
22 balanced. A detailed analysis of the Pluronic/SAIL micelle density profiles showed that the
23 phosphonium head groups were positioned inside the micelle core, whereas smaller imidazolium
24 head groups were placed much closer to the hydrophilic PEG corona, leading to a distinct effect
25 on the cloud point temperature for those two classes of SAIL. Herein, the phosphonium-based
26 SAIL induces a lower repulsion between neighbouring micelles than the imidazolium-based
27 SAILS, resulting in a less pronounced increase of the CPT. The model presented in here offers, for
28 the first time, an intuitive and powerful tool to unravel the complex thermo-response behaviour of
29 Pluronic and SAIL mixtures and support the design of tailor-made thermal controlled solvents.

30

1
2
3
4
5
6
7
8
9
10
11
12
13
14
15
16
17
18
19
20
21
22
23
24
25
26
27
28
29
30
31
32
33
34
35
36
37
38
39
40
41
42
43
44
45
46
47
48
49
50
51
52
53
54
55
56
57
58
59
60

1 **Keywords:** coarse-grain computer model, molecular dynamic simulations, micellar self-assembly,
2 Pluronics and ionic liquid mixtures

3

1. Introduction

Triblock copolymers, also known as Pluronics or Poloxamers, are emerging as promising biocompatible candidates for the development of tuneable and integrated purification platforms as evidenced by their increasing application in the recovery of value-added compounds such as pharmaceuticals,¹ biomolecules² and metals³ amongst others. Pluronics are thermo-responsive copolymers constituted by units of poly(oxyethylene)-poly(oxypropylene)-poly(oxyethylene) - $(EO)_n(PO)_m(EO)_n$ ⁴ or poly(oxypropylene-poly(oxyethylene)- poly(oxypropylene) - $(PO)_m(EO)_n(PO)_m$ ⁵. They present well-known lower critical solution temperature (LCST) behaviour, allowing at the reversible formation of aqueous micellar two-phase systems (AMTPS) by temperature adjustment, simplifying the process development and decreasing the necessity of large quantities of a tertiary compound to promote phase separation. The presence of both EO and PO units allows to fine tune the amphiphilic properties of Pluronics.⁶ The latter aggregate in aqueous solutions to form micelles constituted by a polypropylene glycol (PPG) hydrophobic core with the polyethylene glycol (PEG) segments arranged outwards to form the hydrophilic corona. Upon temperature increase, the PPG hydrophobic effect becomes stronger while the PEG segments dehydrate due to conformational changes in the EO groups, resulting in a two-phase separation at a temperature known as the cloud point.⁶ The versatility of Pluronics as solvents stems from this self-organisation, which is influenced by the ratio of PO to EO units, the PO to EO sequence (normal and reverse Pluronics), and the molecular weight.⁷

Through judicious adjustment of the biphasic environment, conditions promoting the selective partition of target compounds versus contaminants can be achieved. One method to enhance selectivity is through the addition of affinity ligands that significantly partition to one phase, thereby modifying its properties and extraction characteristics.⁸ Ionic liquids (ILs) are promising candidates as affinity ligands due to their ability to solvate a wide range of compounds (polar and apolar) and to act either as a solvent or a catalyst. Surface active ILs (SAILs) are a subset of ILs, with either the cation or anion possessing an alkyl chain longer than six carbon atoms allowing it to self-aggregate in aqueous solutions.⁹ The incorporation of small quantities of SAILs into micellar systems overcomes the major issues traditionally associated with ILs, namely their cost and viscosity. Furthermore, Dong et al.¹⁰ showed that imidazolium-based SAILs can have a better performance than conventional cationic surfactants with lower concentrations required to promote a similar effect. However, studies on the incorporation of SAILs into mixed micelles with both

1
2
3 1 ionic and non-ionic surfactants reveal the marked variability in the resulting properties of the
4 system compared to its pure components, including its cloud-point.^{9,11–20} A deeper understanding
5
6
7 3 of the molecular-scale interactions controlling these complex systems often remains lacking.

8 4 In spite of the individual advantages of Pluronics and SAILs, only a few reports are available on
9
10 5 the effect of ILs on Pluronics, either with short or long alkyl side chain ILs. They are mainly
11
12 6 focused on the influence of SAILs in small concentration ranges, focusing on the critical micelle
13
14 7 concentration (CMC), the critical micellization temperature (CMT) and/or the micelle size. Higher
15
16 8 concentrations required for extraction purposes are often not considered in these studies despite
17
18 9 the pronounced effect of concentration and nature of each compound on the phase behaviour,
19
20 10 namely on the formation of micelles and long range ordered structures, which have different
21
22 11 thermal responses. A detailed knowledge of the molecular scale interactions driving the self-
23
24 12 assembly of these mixtures is of great importance to design and expand the range of thermal
25
26 13 responsive copolymer-SAILs systems. In this respect, computer simulations can rationalize
27
28 14 available experimental data and provide a platform for the inexpensive screening of potential
29
30 15 systems. Our group recently developed a coarse-grain (CG) model for molecular dynamics (MD)
31
32 16 computer simulations of Pluronic aqueous solutions.⁷ The model captured the complexities of
33
34 17 Pluronic micelle formation and the influence of the PPG content, the PEG to PPG ratio or the
35
36 18 Pluronic molecular weight on the cloud point temperature. As such, it provides a valuable
37
38 19 framework to study the influence of SAIL addition to Pluronic aqueous solutions on the thermal
39
40 20 response of the system and complement existing experimental studies.^{12,19–29}

41 21 In this work four selected Pluronics were studied in conjunction with imidazolium and
42
43 22 phosphonium-based SAILs to determine the influence of the ILs as additives on the cloud points
44
45 23 and thermo-responsiveness of the system. Both normal (PEG-PPG-PEG) and reverse (PPG-PEG-
46
47 24 PPG) Pluronics were studied as these structural changes induce major micelle surface variations
48
49 25 from star-like to flower-like shaped micelles, respectively, as well as the occurrence of physical
50
51 26 cross linkage between reverse Pluronic micelles.⁷ Furthermore, the effect of the polymer molecular
52
53 27 weight and PPG to PEG ratio in mixed systems was also assessed. Finally, the influence of the
54
55 28 SAILs cationic alkyl chain length and the nature of the cation, namely imidazolium or quaternary
56
57 29 phosphonium, on the thermo-responsive properties of the system was determined. In doing so, the
58
59 30 conclusions obtained herein can be extended to the application, understanding and design of
60

1
2
3 1 Pluronic-based responsive formulations of relevance for the development of sustainable and
4 integrated separation systems.
5
6
7 3

8 4 **2. Methods**

9 5 *2.1. Experimental Details*

10 6 All studied triblock copolymers studied in this work were purchased from Sigma-Aldrich,
11 7 namely Pluronic L-31, L-35, 31R1 and 10R5 (see **Table S1**). Both the imidazolium: 1-decyl-3-
12 8 methylimidazolium chloride - [C₁₀mim]Cl (> 98 wt%), 1-dodecyl-3-methylimidazolium chloride
13 9 - [C₁₂mim]Cl (> 98 wt%) and 1-methyl-3-tetradecylimidazolium chloride - [C₁₄mim]Cl (> 98
14 10 wt%), and the phosphonium-based SAIL, represented by tributyltetradecylphosphonium chloride
15 11 - [P_{4,4,4,14}]Cl (95 %), were acquired at Iolitec (Ionic Liquid Technologies, Heilbronn, Germany).
16 12 McIlvaine buffer (0.18 M) at pH 7.0 was used as solvent, being composed of sodium phosphate
17 13 dibasic heptahydrate (purity ≥ 99%) and citric acid monohydrate (purity ≥ 99%), which were
18 14 obtained from Panreac AppliChem.

19 15 The cloud point determination was established in McIlvaine buffer solutions, since this is the
20 16 medium of preference to work with pH sensitive or labile biomolecules, and at copolymer
21 17 concentrations ranging from 0.5 to 17.5 wt% and SAIL concentrations of 0.3 wt%. For each
22 18 system, three replicas were determined, and the average value calculated. The cloud points were
23 19 measured through the visual determination of the onset turbidity of a solution heated in a
24 20 temperature controlled water bath with an error of ± 0.01 °C following a methodology described
25 21 elsewhere.^{30,31} The full results are shown in **Figure S1**.
26
27
28
29
30
31
32
33
34
35
36
37
38
39
40

41 23 *2.2. Simulation Details*

42 24 The CG models for Pluronics,⁷ phosphonium³² and imidazolium³³ ILs used in this work were
43 25 successfully developed, validated and discussed in recent publications by the authors, and are
44 26 shown in **Figure 1**. They are based on the MARTINI framework,³⁴ with appropriate adaptations
45 27 for the specific systems studied here. the applicability and transferability of the MARTINI CG
46 28 approach has been widely documented in the recent literature,^{35–37} and the reader is referred to
47 29 those studies for additional details. Simulations were carried out with the four Pluronics, 10R5,
48 30 31R1, L-35 and L-31 at several concentrations, with and without the addition of SAILs. For the
49 31 latter, we considered two imidazolium compounds with different cation alkyl chain lengths, as
50
51
52
53
54
55
56
57
58
59
60

1 well as one representative of phosphonium SAILs. All possible combinations were tested with 1
2 wt% of Pluronic and 0.3 wt% of [C_nmim]Cl (n=10, 14) and [P_{4,4,4,14}]Cl, at the cloud point
3 temperatures determined experimentally. In total, 16 MD simulations for different Pluronic/SAIL
4 mixtures of at least 3.0 μs of simulation time were carried out, the details of which can be consulted
5 in **Table S2**. To more clearly understand the complex interactions taking place during the initial
6 stages of the self-assembly of Pluronic/SAIL micelles, we have also carried out a series of MD
7 simulations at room temperature (25°C) for selected concentrations, as summarised in **Table S3**.
8 For each Pluronic, these included the reference system without SAIL and two systems with 0.3
9 wt% of [C₁₄mim]Cl or [P_{4,4,4,14}]Cl. The simulation times were also up to 3.0 μs.

10 All MD simulations were carried out with the Gromacs 5.1.4 package³⁸ adopting the leapfrog
11 algorithm³⁹ to integrate the equations of motion with a time step of 10 fs. The potential energy
12 function encompassed the bond stretching, angle bending and dihedral torsion for bonded
13 interactions, and Lennard–Jones (LJ) and Coulombic terms for non-bonded interactions. The
14 force-switch modifier was employed in the LJ interactions with the energy decaying smoothly to
15 zero between 1.0 and 1.2 nm. The Verlet algorithm⁴⁰ was used in combination with the neighbour
16 list updated every 20 steps. The cut-off function with the Potential-Shift-Verlet modifier was used
17 for long-range Coulombic interactions with a cut-off radius of 1.2 nm. Long-range Coulombic
18 interactions were evaluated through particle mesh Ewald (PME).⁴¹ All bonds were constrained by
19 the LINCS algorithm.⁴² Cubic boxes with periodic boundary conditions were used placing all the
20 molecules randomly, followed by an equilibrium process described previously.⁷ Afterwards, all
21 systems were run for 0.5 μs of simulation time in the NpT ensemble. Unless otherwise stated, the
22 reported simulation time was the number of steps multiplied by the nominal time step (10 fs). The
23 temperature was fixed with the velocity-rescaling thermostat⁴³ in the equilibration stage and the
24 Nose-Hoover thermostat^{44,45} in the production runs, to ensure adequate ensemble sampling. The
25 pressure coupling was considered as isotropic and the pressure was fixed at 1 bar using the
26 Parrinello–Rahman barostat.⁴⁶ The MD simulations were visualised using the VMD software
27 package.⁴⁷ The density profile, micelle distribution and the aggregation number were obtained
28 using an in-house code^{7,48,49} based on the Hoshen–Kopelman cluster-counting algorithm.⁵⁰

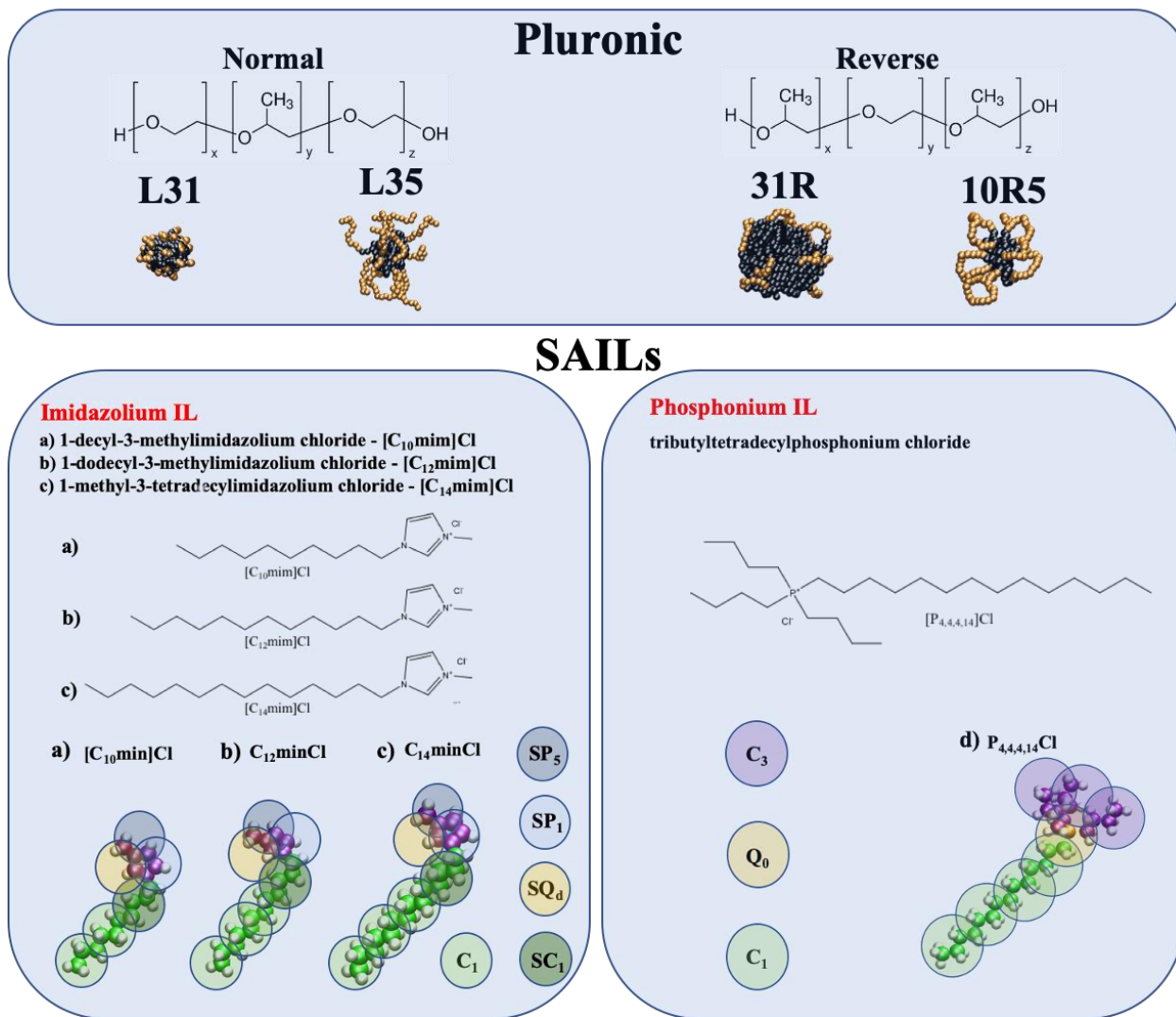


Figure 1. Structure of the Pluronic and SAILs CG model used in this work. The Pluronic micelle pictures were taken from the MD simulations carried out previously.⁷ The PPG and PEG in the Pluronic micelles are in black and orange colour, respectively. In the bottom, the imidazolium-based ionic liquids were modelled by using a 3:1 mapping (3 heavy atoms per CG bead), labelled with the prefix S, with a size of $\sigma = 0.43$ nm, whereas regular sized $\sigma = 0.47$ nm beads were used to map the phosphonium-based ionic liquid. The colour code is as follows; green is for the most apolar character, light orange for charged centers, purple for medium apolar behaviour, light blue for the lowest polar character and finally the dark blue colour was chosen for the most polar regions of the ionic liquid.

3. Results and discussion

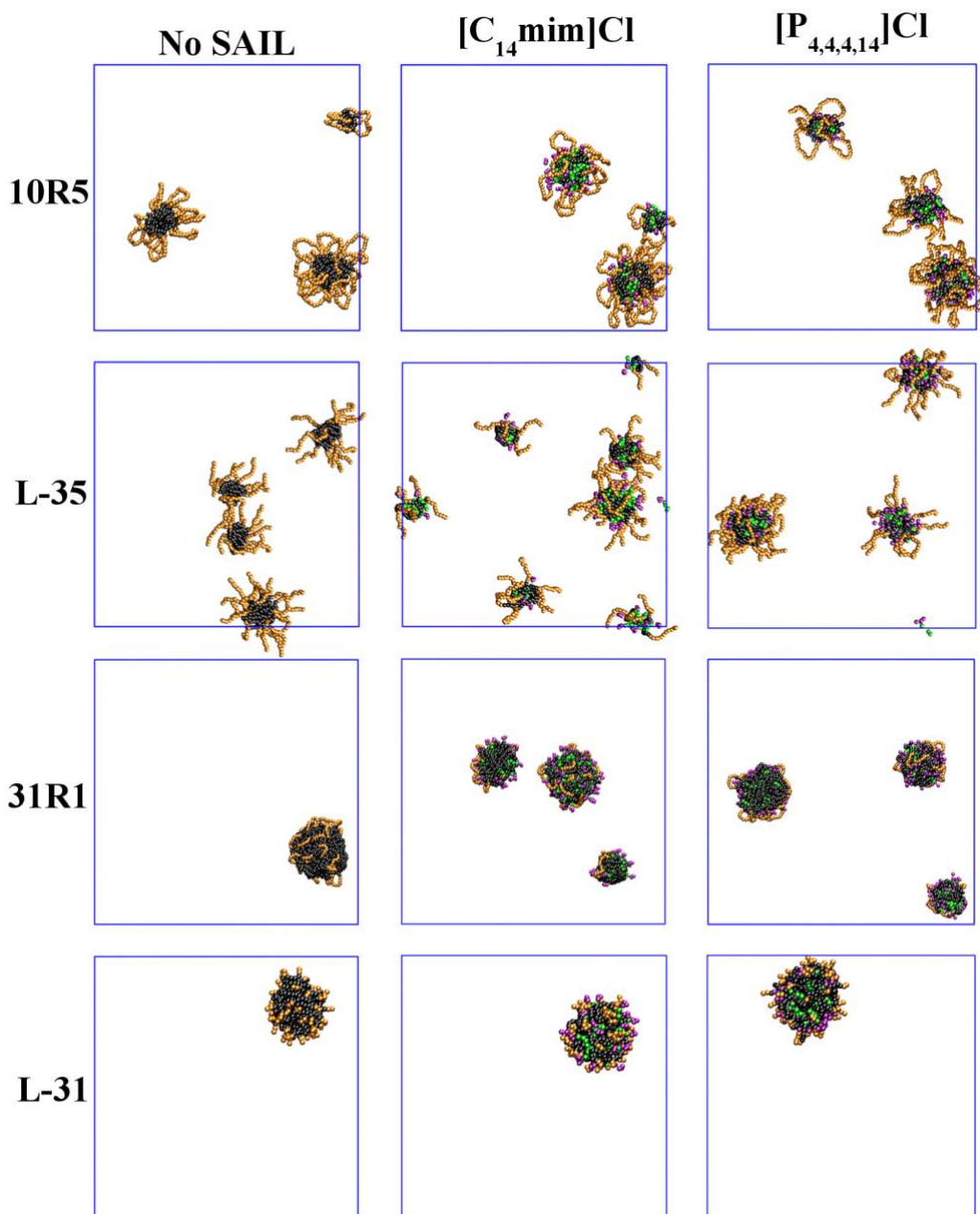
3.1 MD simulations of self-assembly in mixed Pluronic-SAIL systems

In a previous paper, a new CG model was developed to provide a microscopic insight into the complex self-assembly of Pluronic surfactants in aqueous solutions.⁷ This CG model was our base line to study the impact of SAILs on the cloud point behaviour of Pluronic systems. Firstly, two Pluronics with the same amphiphilic character (~ 50 wt% of PEG) were compared, namely the star-like L-35 and the flower-shape 10R5, to evaluate the effect of the micelle PEG surface shape. Then, two normal Pluronics with the same PPG content but different PEG content, L-31 and L-35, were analysed to elucidate how the PEG moiety size affects the formation of mixed micelles. Finally, the reverse Pluronic 31R1 with ~ 10 wt% of PEG was also analysed and compared with the 10R5, which has five times more EG units.

The room temperature simulations (see **Table S3**) provide an interesting picture of the initial stages of self-assembly in these Pluronic/SAIL systems. To ensure that the micelle equilibrium is reached, the total potential energy (E_{tot}) was monitored. The energy decreased during the initial micelle formation until reaching a plateau as soon as the micellar growth stops taking place. After this, only small fluctuations were observed as shown in **Figure S2** for the Pluronic aqueous solutions and their Surface-Active Ionic Liquid (SAIL) mixtures at 298K. This procedure was followed in our previous study on Pluronic-water solutions,⁵¹ where the E_{tot} plateau region was reached after 3 μs of simulation time and the simulated micelle size distributions agreed with the results of experimental measurements. This suggests that the system had been successfully equilibrated and gives us confidence that the same is true for the simulations incorporating SAIL in the Pluronic aqueous solutions. **Figure S2** emphasizes that the equilibrium was attained after 1 μs in all of the systems except 31R1 which required 2 μs due to the high molecular weight (this system includes ~1.5 million CG water beads). Additionally, to ensure that our simulations are free from any system-size effects, the 10R5 systems containing 60 Pluronic moieties (twice the normal size) were simulated over 3 μs for the Pluronic aqueous solutions and their SAIL mixtures, concretely with [P_{4,4,4,14}]Cl and [C₁₄mim]Cl. **Table S4** shows the number of micelles, the aggregation number and micelle diameters for those simulations. Very good agreement was found between small and large systems. Additionally, the double-sized 10R5/water system was run for 9 μs , and we observed that the micelle distribution was unchanged between 4 μs and 9 μs . The E_{tot} for the double-sized systems was monitored and compared with results obtained with the small systems. Both systems

1 followed a similar pattern, with the smaller system reaching equilibrium after $\sim 1 \mu\text{s}$ (solid lines)
2 whereas the double-sized systems (dashed lines), required $2 \mu\text{s}$ at least, as shown in **Figure S3**. To
3 further ensure that the micelle distribution equilibrium was reached the aggregation number (N_a)
4 vs simulation time is shown in **Figure S4** for all systems at 25°C . It can be seen that between 2 and
5 $3 \mu\text{s}$, the N_a barely changes, reaching a Plateau, which suggest that micelles have reached their
6 equilibrium size distribution.

7 The final simulation snapshots are shown in **Figure 2**, displaying the micelle formation with
8 and without the addition of SAIL. It can be clearly seen that in the presence of SAIL, hybrid
9 micelles containing both Pluronic and SAIL molecules were formed. This is because both
10 components have amphiphilic properties and at these dilute conditions, both have a tendency to
11 form micellar aggregates. A key difference between the two amphiphiles is that SAIL molecules
12 are charged, while Pluronics are neutral. As we will discuss shortly, this introduces a Coulombic
13 character into the otherwise neutral Pluronic micelles, with some interesting consequences on the
14 cloud point behaviour.



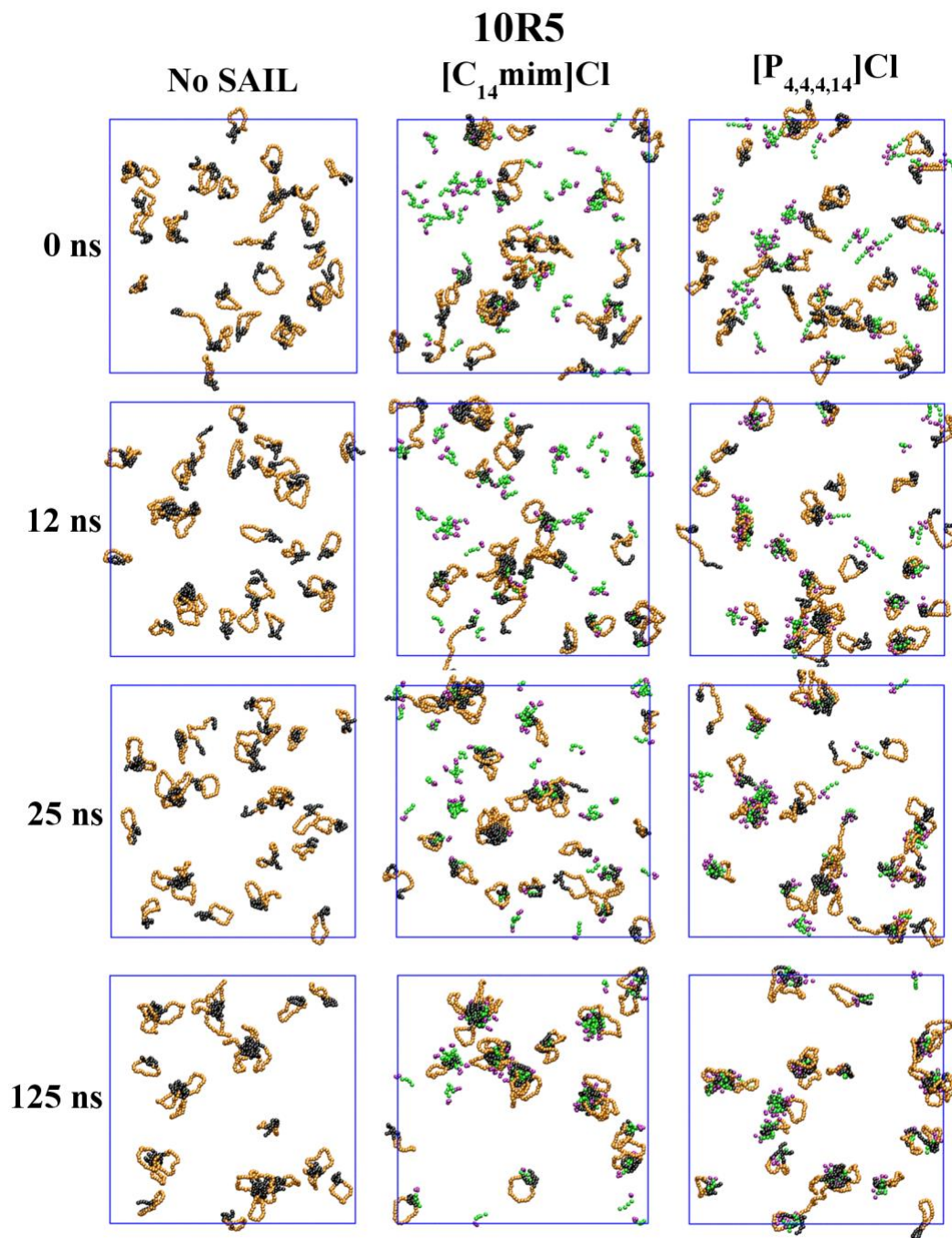
1
2
3
4
5
6
7
8

Figure 2. MD simulation snapshots after 3.0 μs of simulation time for 10R5, L-35, 31R1 and L-31 at 1 wt% in aqueous solutions (left column) and their mixtures with 0.3 wt% of $[C_{14}mim]Cl$ and $[P_{4,4,4,14}]Cl$, (middle and right columns, respectively). The temperature was fixed to 25°C. The colour code is as follows: for Pluronics, the PPG and PEG are in black and orange, respectively; for SAILs, the hydrophobic alkyl-chain tail is green whereas the imidazolium ring in $[C_nmim]Cl$ and the butyl head groups in $[P_{4,4,4,14}]Cl$ are coloured in purple. Water and chloride ions were removed for clarity.

1
2
3
4
5
6
7
8
9
10
11
12
13
14
15
16
17
18
19
20
21
22
23
24
25
26
27
28
29
30
31
32
33
34
35
36
37
38
39
40
41
42
43
44
45
46
47
48
49
50
51
52
53
54
55
56
57
58
59
60

1 Given the amphiphilic properties of both components, it is interesting to examine the
2 mechanism of micelle self-assembly in more detail. The self-assembly processes can be followed
3 closely in the MD simulation movies **SM1** to **SM4** (one for each Pluronic) which can be found in
4 the Supporting Information. In **Figure 3**, we show several snapshots of the initial stages of
5 equilibration in solutions of 10R5 Pluronic, with and without SAIL. We focused on the two classes
6 of ionic liquids, imidazolium and phosphonium, with the same alkyl chain length. As previously
7 described,⁷ in the solution without SAIL, individual 10R5 molecules start by forming small loops
8 whereby the two hydrophobic PPG ends join together. Shortly after that, the loops aggregate into
9 small micelles, which eventually fuse together to form the equilibrium micelle distribution. When
10 SAILs are present in the solution (middle and right columns in **Figure 3**), the 10R5 loops coexist
11 with small aggregates (proto micelles) of the SAIL that are also formed quickly at the beginning
12 of the simulation. As the self-assembly progresses, some of the isolated Pluronic molecules are
13 incorporated in growing SAIL aggregates, and vice-versa. This originates two classes of hybrid
14 micelles, one dominated by Pluronics with some adsorbed SAIL (we call these Pluronic/SAIL
15 micelles) and another class dominated by SAIL with some adsorbed Pluronics (i.e. SAIL/Pluronic
16 micelles). Subsequent micelle fusion gives rise to a small number of larger hybrid micelles that
17 contain both amphiphilic components, as shown for 10R5 + [C₁₄mim]Cl and 10R5 + [P_{4,4,4,14}]Cl
18 in **Figure 2**.

19 The self-assembly mechanism described above is similar, regardless of the type of SAIL that is
20 present. This can be seen by comparing the middle and right columns in **Figure 3**. The main
21 difference is that the initial SAIL aggregates are somewhat larger for [P_{4,4,4,14}]Cl than for
22 [C₁₄mim]Cl, due to the slightly more hydrophobic head of the former. Furthermore, the mechanism
23 is very similar for L-35 (**Figure S5**), except for the fact that the Pluronic is normal and not reverse,
24 thus the chains initially form “knots” instead of loops – the effect of SAIL is, however,
25 qualitatively the same. **Figure S6** shows a close-up for this system, where we can easily discern
26 individual SAIL and Pluronic micelles formed in the early stages of self-assembly. Hybrid
27 SAIL/Pluronic and Pluronic/SAIL aggregates can also be discerned. It is important to note that for
28 both 10R5 and L-35 systems, the evolution of the average aggregation number with time is very
29 similar in the solutions with and without SAIL (**Figures 3, S4** and **S5**) – at any given time, there
30 is approximately the same number of micelles in the three solutions.



47
48
49
50
51
52
53
54
55
56
57
58
59
60

Figure 3. Detailed description of the initial stages of micelle formation in 10R5 aqueous solutions (left column) and their mixtures with $[C_{14}mim]Cl$ (middle column) and $[P_{4,4,4,14}]Cl$ (right column). The temperature was fixed to 25°C. The colour code is the same as in **Figure 2**.

1
2
3
4
5
6
7
8
9
10
11
12
13
14
15
16
17
18
19
20
21
22
23
24
25
26
27
28
29
30
31
32
33
34
35
36
37
38
39
40
41
42
43
44
45
46
47
48
49
50
51
52
53
54
55
56
57
58
59
60

1 This picture changes significantly when we consider the two Pluronics with larger PPG
2 segments, 31R1 (**Figure 4**) and L-31 (**Figure S7**). In these cases, the Pluronic self-assembly in the
3 reference system without SAIL takes place much faster, due to the large driving force for
4 aggregation caused by the long PPG chains. As a consequence, large Pluronic micelles are already
5 formed after a few tens of nanoseconds (see left column of **Figure 4**). In contrast, this does not
6 happen in the solutions with SAIL, where instead we observe a self-assembly mechanism that is
7 rather similar to that of 10R5 and L-35 –initially small micelles of Pluronic and SAIL are formed,
8 followed by much slower processes of micelle growth and micelle fusion. In fact, even after 125
9 ns, there are still micelles of pure SAIL in the solution (see bottom-right panel of **Figure 4**). One
10 can conclude that one of the effects of the addition of SAIL in these systems is that micelle fusion
11 becomes much less favourable, which slows down the self-assembly process.

12 In **Figure 5**, we show a more detailed picture of the hybrid micelles formed in the
13 Pluronic/SAIL aqueous solutions. As we can see, the Pluronic/SAIL micelles have quite similar
14 structures to the pure Pluronic micelles (compare with the examples shown in **Figure 1** and those
15 previously reported).⁷ The ionic liquid molecules are embedded within the PPG core, with the
16 charged head groups protruding into the PEG corona region. The SAIL/Pluronic micelles (right-
17 hand side of **Figure 5**) also show a similar structure to pure SAIL micelles,^{33,52} with a hydrophobic
18 core composed of the alkyl chains and most of the polar heads at the surface. In this case, the PPG
19 moieties of the Pluronics are embedded in the alkyl core, while the hydrophilic PEG chains
20 protrude outward into the aqueous solution. It is also apparent that the arrangement of the Pluronic
21 chains in the SAIL/Pluronic micelles is rather disordered, particularly when compared to the pure
22 Pluronic micelles.

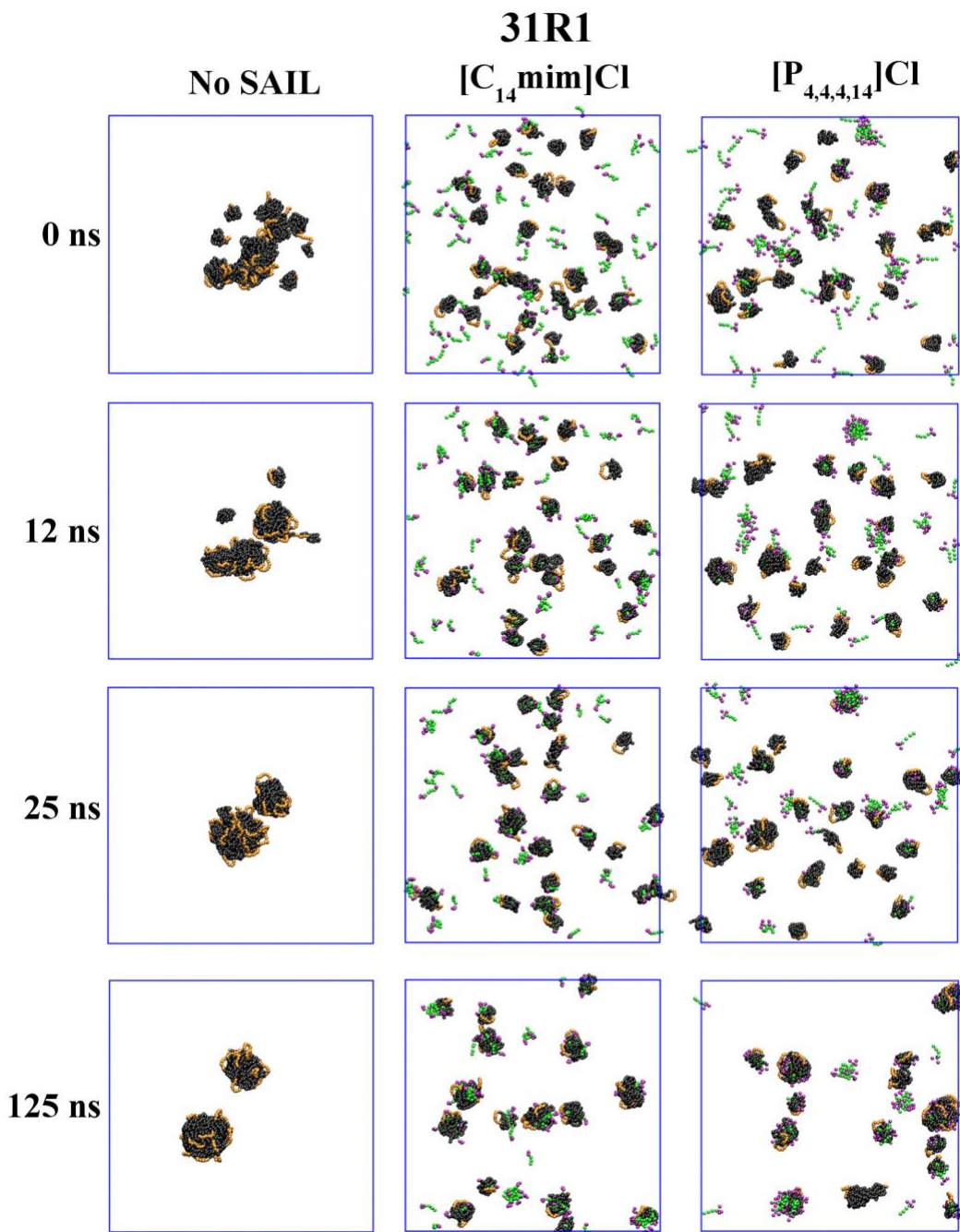
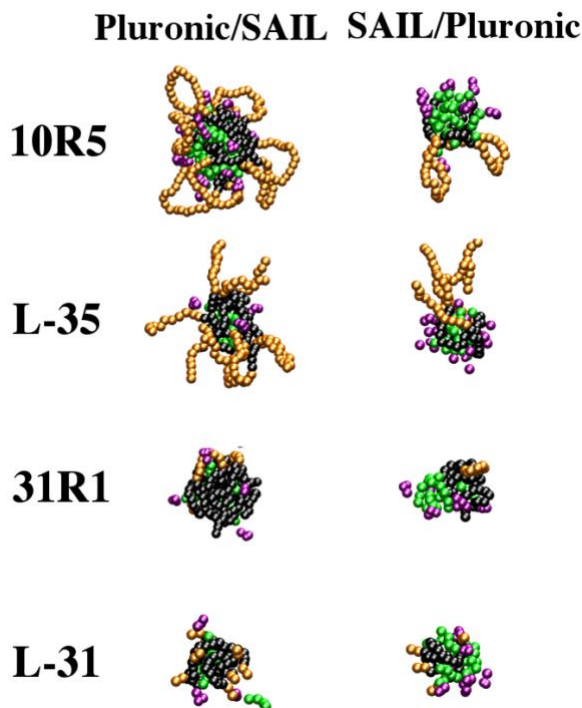


Figure 4. Detailed description of the initial stages of micelle formation in 31R1 aqueous solutions (left column) and their mixtures with $[C_{14}mim]Cl$ (middle column) and $[P_{4,4,4,14}]Cl$ (right column). The temperature was fixed to 25°C. The colour code is the same as **Figure 2**.



26
27
28
29
30

Figure 5. Examples of hybrid Pluronic/SAIL and SAIL/Pluronic micelles found in the MD simulations for 10R5, L-35, 31R1 and L-31 Pluronics mixed with SAILs. The colour code is the same as in **Figure 2**.

31
32
33
34
35
36
37
38
39
40
41
42
43
44
45
46
47
48
49
50
51
52
53
54
55
56
57
58
59
60

As mentioned before, the incorporation of SAIL molecules into the Pluronic micelles introduces a charged character at the micelle surface. This can be seen in the average radial density profiles of the Pluronic/SAIL micelles, an example of which, for the L-31 Pluronic, is shown in **Figure 6**. Similar density profile plots for the other 3 systems can be found in the Supporting Information (**Figures S8-S10**). In all cases, the charged regions of the SAIL cations arrange themselves near the interface between the PPG core and the PEG corona. The chloride counterions, on the other hand, arrange themselves in a diffuse layer that is mostly outside the core of the micelle, as observed for typical cationic surfactant micelles.⁴⁸ This means that inter-micellar repulsion due to the electrical double layer will hinder micelle fusion, which explains why this process was so much slower in Pluronic/SAIL solutions (**Figure 4**). This charged character of the mixed micelles will also have a pronounced effect on the onset of the cloud point, as discussed in section 3.2.

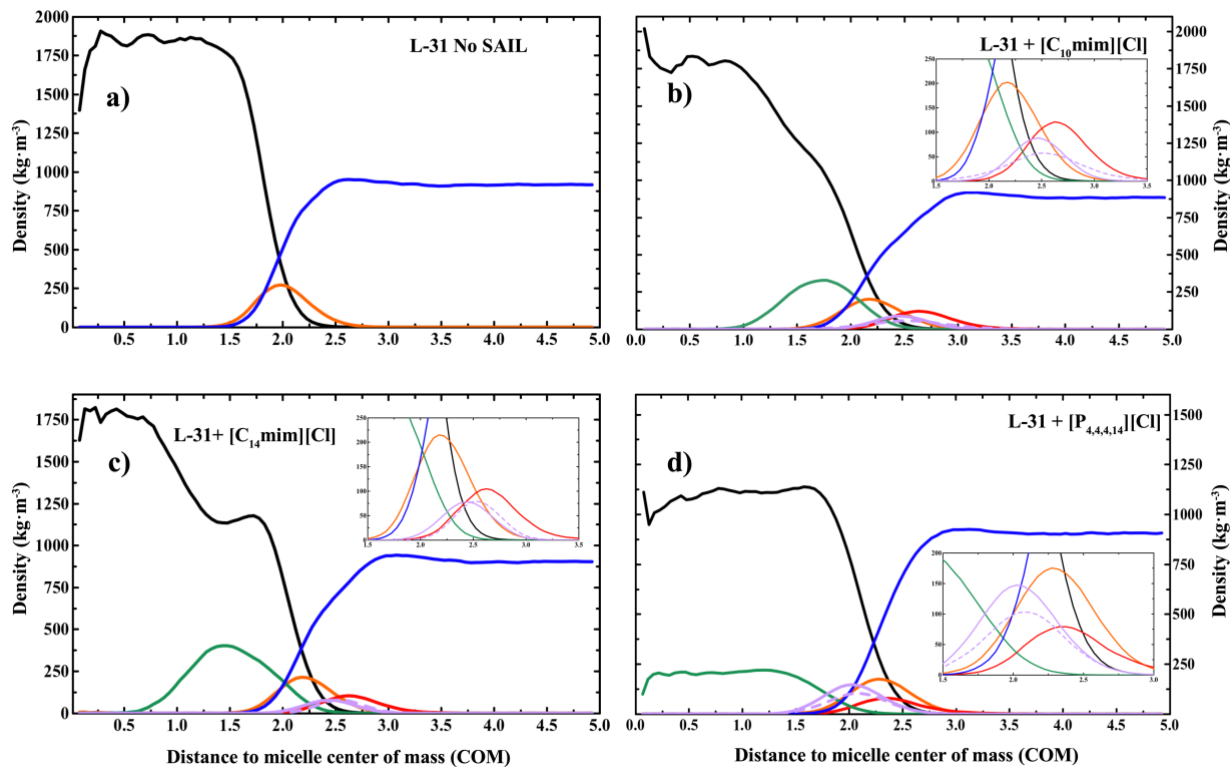
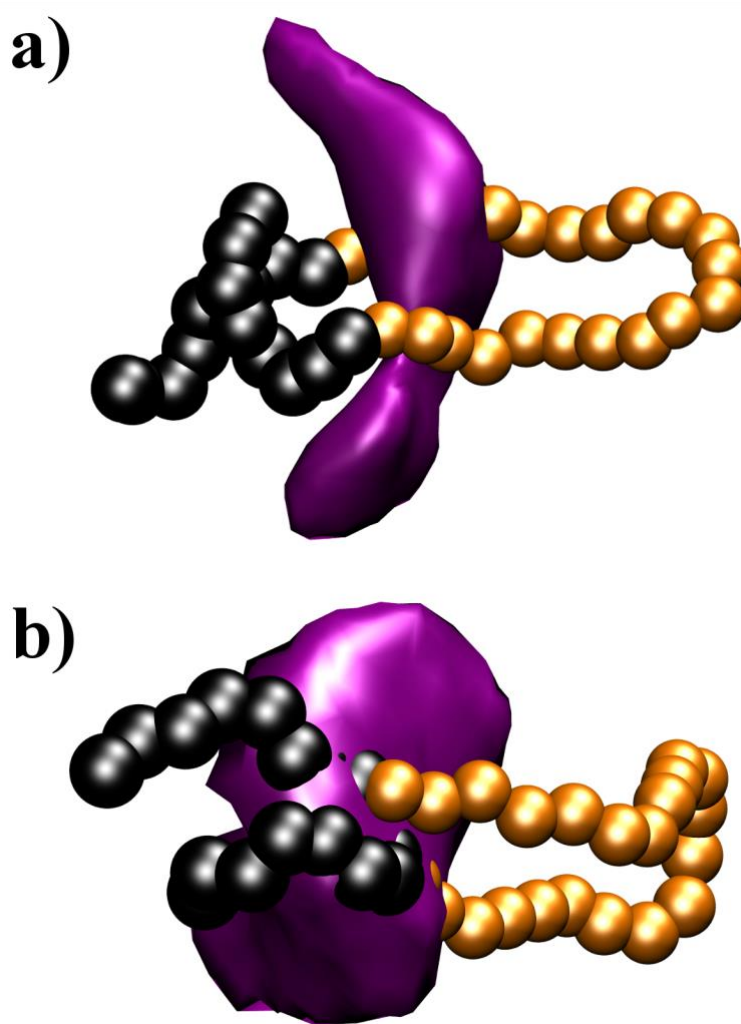


Figure 6. Micelle density profiles for L-31 solutions without SAILs (a) and after addition of $[C_{10}\text{mim}]\text{Cl}$ (b), $[C_{14}\text{mim}]\text{Cl}$ (c) and $[P_{4,4,4,14}]\text{Cl}$ (d). The colour code is as follows: SAIL alkyl-chain tails in green, SAIL head groups in purple, water in blue, chloride counter ions in red, PEG micelle corona in orange and PPG micelle hydrophobic core in black. The dashed purple line shows the profile for the charged site of the SAIL head group, multiplied by a factor of 3 for ease of visualization. The insets show a blow up of the head-group region for the systems with SAIL.

Interestingly, there are some subtle structural differences in micelles formed with different SAILs. The much bulkier nature of the phosphonium head group gives it a somewhat more hydrophobic character. As a consequence, the corresponding peaks tend to be on the inner side of the micelle surface, closer to the PPG core (compare the position of the purple lines in the insets of **Figure 6**). In particular, the charged site peak is well to the left of the peak corresponding to the PEG corona, indicating that it is somewhat “buried” within the core. In contrast, the smaller, and more hydrophilic, imidazolium head groups tend to protrude further into the PEG corona, being more exposed to the solution medium. In fact, for both imidazolium cations, the peak of the charged group profile is to the right of the PEG corona, and well outside of the PPG core. This observation is confirmed by examining Surface Distribution Functions (SDF) of the charged bead of each SAIL around the interface between the PEG and PPG groups of the Pluronic (**Figure 7**).

1 These SDFs essentially show the average surface of charge around each Pluronic molecule in a
2 hybrid micelle. As can be seen, the surface moves closer to the PPG groups with the phosphonium
3 SAIL when compared to the imidazolium counterpart with the same chain length (**Figures 7a** and
4 **7b**). This means that systems containing imidazolium will exhibit more pronounced effects of
5 inter-micellar repulsion. The same structural differences were observed for all other Pluronic
6 systems (see **Figures S8-S10**). However, the effect is more pronounced, in relative terms, for the
7 Pluronics with less PPG and more PEG because the micelles become significantly smaller and the
8 adsorption of SAIL leads to a larger perturbation of the surface structure.
9



10
11 **Figure 7.** Surface Distribution Functions for the charged IL cation site with respect to the PEG to PPG interface
12 in the 10R5 system with: (a) [C₁₄mim]Cl; (b) [P_{4,4,4,14}]Cl. The micelle interface was defined by considering the three
13 PEG beads closest to the PPG group as a reference for calculating the SDFs. An example configuration of a single

1
2
3 1 Pluronic chain is also shown for comparison. The PEG sites are in orange, the PPG in black and the cation charged
4 2 site probability surface in purple.
5
6 3

7
8 4 Comparing micelles containing [C₁₀mim]Cl and [C₁₄mim]Cl, the average location of the head
9 5 group is nearly the same. However, the [C₁₀mim]Cl system shows a much broader distribution,
10 6 suggesting that the arrangement of the SAIL at the micelle surface is significantly more disordered
11 7 than in the case of [C₁₄mim]Cl. This suggests that the effects of inter-micellar repulsion will not
12 8 be as pronounced with the shorter-chain IL cation. Interestingly, this difference was only
13 9 significant for the L-31 Pluronic –for the other three systems, the [C₁₀mim]Cl and [C₁₄mim]Cl are
14 10 almost indistinguishable (**Figures S5-S7**). This is possibly due to the extremely small PEG corona
15 11 in L-31, which makes it harder for the shorter IL cation to adopt a very ordered arrangement at the
16 12 surface.
17
18
19
20
21
22
23
24

25 14 *3.2 Thermo-responsive behaviour of mixed Pluronic-SAIL systems*

26
27 15 As previously discussed in detail, triblock copolymers display a thermo-responsive behaviour
28 16 in aqueous solutions.⁷ The PPG:PEG ratio plays an important role in controlling the cloud point,
29 17 since it determines the balance between hydrophobic and hydrophilic interactions. For example,
30 18 when the PPG:PEG ratio is increased from 10R5 to 31R1, the micelles become much larger due
31 19 to the hydrophobic interactions being stronger than the hydrophilic ones, and this leads to a much
32 20 lower cloud point temperature.⁷ Furthermore, the differences in structure between normal (PEG-
33 21 PPG-PEG) and reverse (PPG-PEG-PPG) Pluronics induce major micelle surface changes from
34 22 star-like to flower-like shaped micelles, respectively (*cf.* **Figure 1**). In reverse Pluronics, above a
35 23 certain concentration, the possibility of physical cross-linking between micelles favours self-
36 24 aggregation, thus, the system requires less energy to coalesce and separate into two macroscopic
37 25 phases than the corresponding normal Pluronic. This is the reason behind the lower cloud points
38 26 observed in Pluronic 10R5 when compared with L-35, both with the same PEG and PPG content
39 27 (50/50 %).
40
41
42
43
44
45
46
47
48

49 28 The complex interactions between non-ionic Pluronics and SAIL cations were studied
50 29 alongside the binodal curves. Above 3 wt% Pluronic concentration, for the low concentration of
51 30 SAIL (0.3 wt%) used in this work, the co-polymer totally dominates the phase behaviour resulting
52 31 in very similar trends for all studied systems, *c.f.* **Figure S1**. As such, our analysis focuses on
53
54
55
56
57
58
59
60

dilute systems since these display the greatest variation in the cloud points with SAIL concentration and type. **Figure 8** summarizes the experimental cloud points for < 5 wt% of Pluronic concentration with 0.3 wt% of SAIL. Imidazolium-based SAILS are represented by $[C_n\text{mim}]\text{Cl}$ ($n = 10, 14$) and phosphonium-based SAIL by $[P_{4,4,4,14}]\text{Cl}$. This selection was made based on previous results in which these SAILS increased the cloud point temperature of non-ionic surfactant mixtures, albeit in markedly different ways.^{30,31}

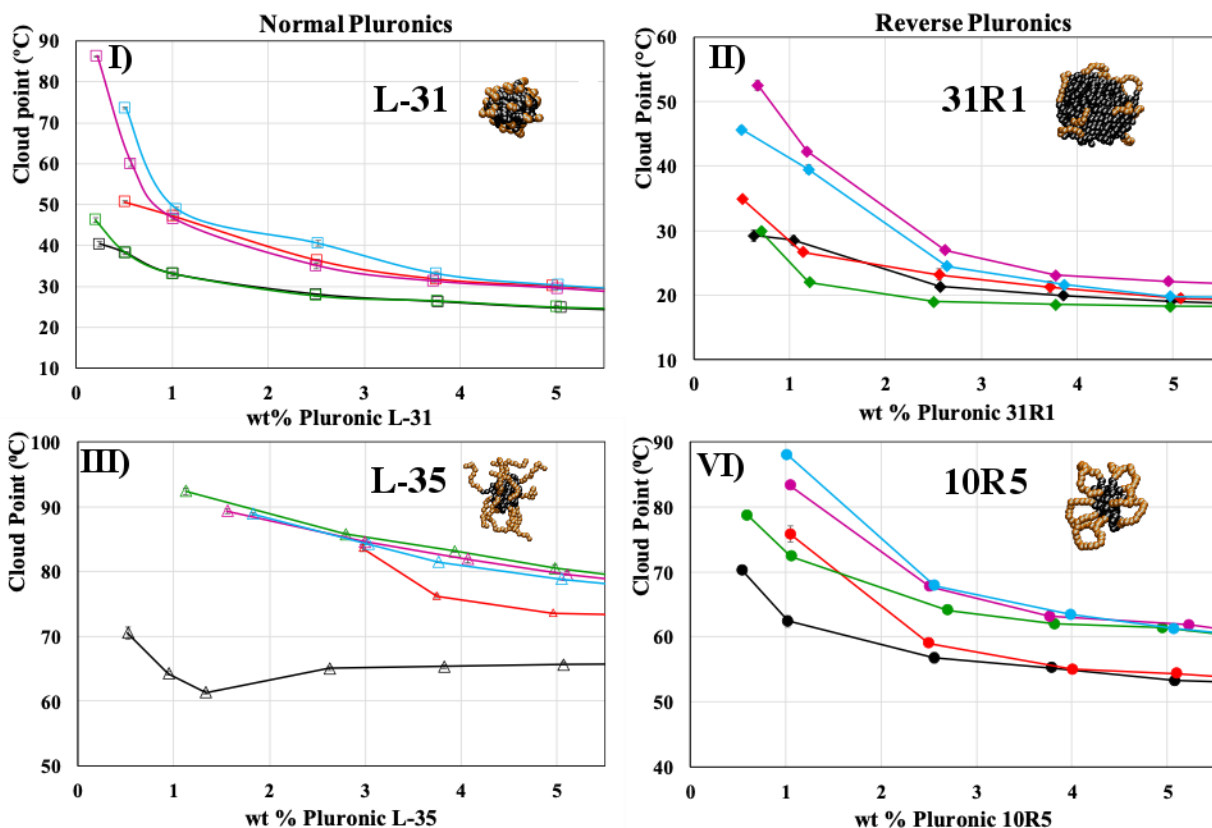
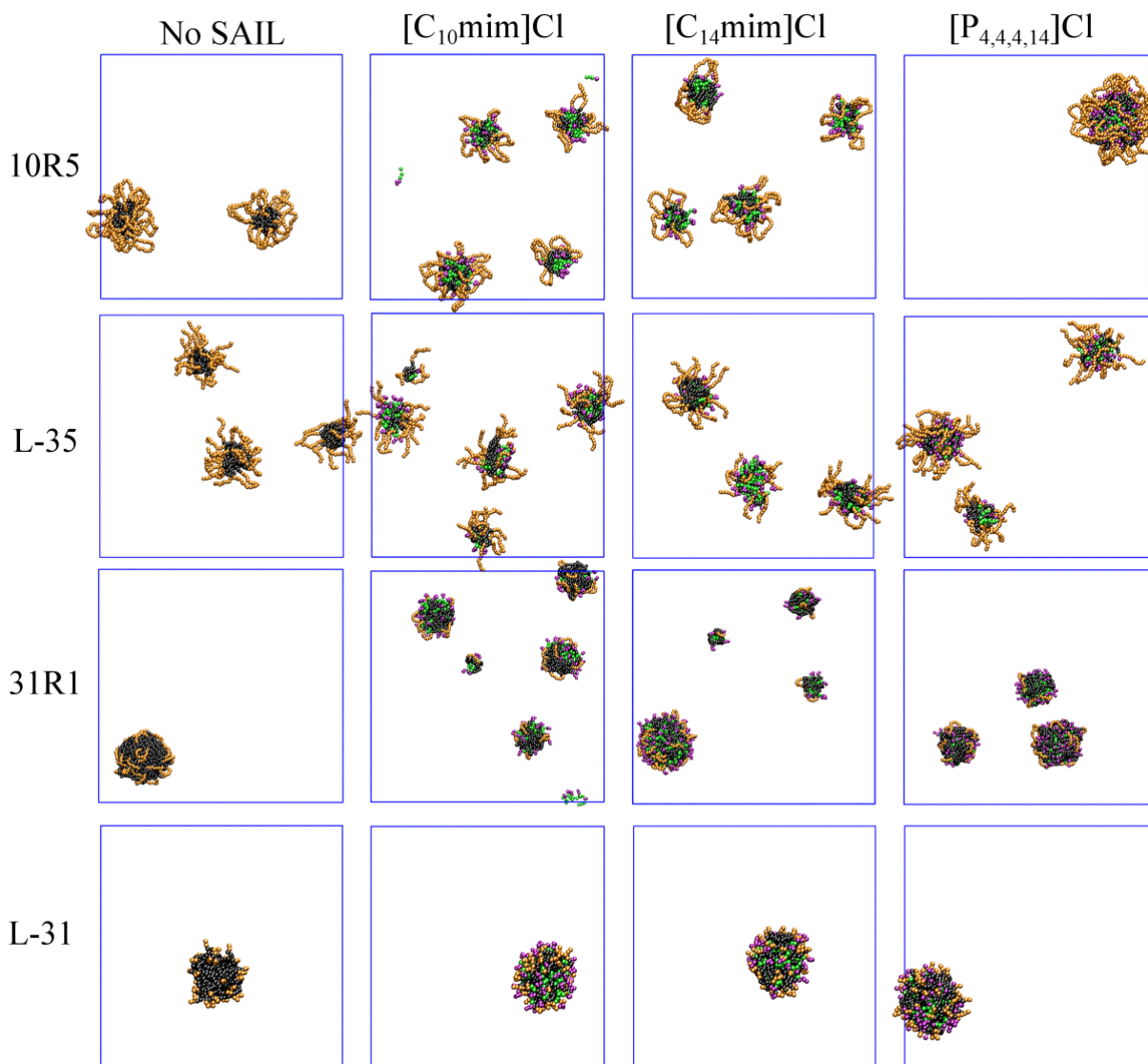


Figure 8. Binodal curves of Pluronic copolymers + 0.3 wt% of SAIL + 0.18 M of McIlvaine buffer pH 7.0. **I**) □, Pluronic L-31. **II**) Δ, Pluronic L-35. **III**) ♦, Pluronic 31R1. **IV**) ●, Pluronic 10R5. The SAILS added to the Pluronic aqueous solutions are: —, $[C_{10}\text{mim}]\text{Cl}$; —, $[C_{12}\text{mim}]\text{Cl}$; —, $[C_{14}\text{mim}]\text{Cl}$; —, $[P_{4,4,4,14}]\text{Cl}$. The black line corresponds to the reference system without SAIL. The error bars are smaller than the symbol size. The inset snapshot micelles were taken from our MD simulations.

In general, the addition of SAIL induces an increase in the Pluronic cloud points, though this effect seems to be dependent on the Pluronic structure. The changes in these cloud points differ from those observed in previous works for mixed AMTPS composed of conventional non-ionic surfactants, namely belonging to the polyoxyethylene alkyl ether family, and SAILS of the $[C_n\text{mim}]\text{Cl}$ family with $n < 8$, for which the cloud point increased with the decrease of the SAIL

1 alkyl side chain length.^{30,31,53} In this work, [C₁₀mim]Cl displayed the lowest impact on the cloud
2 points, in some cases with no influence at all (see, *e.g.* the Pluronic L-31 binodal curve).
3 Conversely, [C₁₀mim]Cl and [C₁₄mim]Cl both behaved similarly, exhibiting the highest cloud
4 point temperatures. The [P_{4,4,4,14}]Cl also induces an increase on the cloud points albeit lower than
5 imidazolium with similar alkyl-chain length ([C₁₄mim]Cl).³¹

6 The experimental cloud point conditions shown in **Figure 8** were reproduced by MD
7 simulations to analyse the thermo-response behaviour of these Pluronic/SAIL mixtures. The
8 Pluronic concentration was 1 wt% since the experimental results exhibited the greater effect with
9 a SAIL concentration of 0.3 wt%. The MD simulation snapshots of the overall systems (see **Table**
10 **S2** for details) after 3.0 μs are shown in **Figure 9**. A detailed view of the micelle formation is
11 shown in the simulation movies (**Films SM5-SM14**; see Supporting Information) of the
12 Pluronic/SAIL systems corresponding to the snapshots of **Figure 9**.



39
40
41
42
43
44
45

Figure 9. MD simulation snapshots after 3.0 μ s for Pluronics 10R5, L-35, L-31 and 31R1 at 1 wt% in aqueous solutions (top row) and their mixtures with 0.3 wt% of [C₁₀mim]Cl, [C₁₄mim]Cl and [P_{4,4,4,14}]Cl (3 lower rows). The temperature was set at the experimental cloud point temperatures shown in **Figure 8** and also displayed in **Table S2**. The colour code is the same as in **Figure 2**.

46
47
48
49
50
51
52
53
54
55
56
57
58
59
60

The competition between Pluronic and SAIL micelle formation as well as the adsorption of the second compound into the formed micelles leads to a rather complex behaviour. It is the balance between each of the individual effects identified in section 3.1 that leads to the different cloud point curves for each system. First of all, with few exceptions, addition of SAIL to an aqueous solution of Pluronics leads to an increase in the cloud point. This is generally caused by the

1
2
3 1 introduction of surface charge (see, *e.g.*, **Figure 7**), which leads to inter-micellar repulsions and
4 makes it more difficult for micelles to aggregate. As a consequence, the onset of the cloud point is
5 raised up to higher temperatures.
6
7

8 4 Another general observation is that phosphonium cations have less impact on the cloud point
9 than imidazolium cations of the same chain length. In fact, the red lines (for phosphonium) in
10 **Figure 8** tend to be located at lower temperatures than the blue lines, corresponding to the
11 imidazolium cation with the same chain length. This shift in temperature with the type of head
12 group is more pronounced for the smaller Pluronic solutions (lower panels in **Figure 8**). This shift
13 is mainly due to the different effects on the micelle structure induced by these two cations. As
14 explained earlier, the phosphonium charged site is much more “buried” inside the PPG core,
15 whereas the smaller imidazolium head group protrudes much more onto the PEG corona. As a
16 consequence, Pluronic micelles with adsorbed imidazolium are more prone to inter-micellar
17 repulsion, resulting in a stronger effect on the cloud point. Furthermore, as seen in **Figure 9**, the
18 systems with [P_{4,4,4,14}Cl] tend to form larger micelles at the CPT compared with [C₁₄mim]Cl, which
19 leads to a more diffuse surface charge.
20
21
22
23
24
25
26
27
28

29 16 The surface effects are less pronounced in Pluronics with larger PPG cores like L-31 and 31R1
30 than in the Pluronics with smaller PPG cores, such as L-35 and 10R5. This is because the onset of
31 the cloud point in the former is much more dominated by hydrophobic effects, so surface effects
32 are less important in relative terms. In the particular case of the L-31 system, both types of SAIL
33 seem to have similar effects on the cloud point (see **Figure 8I**). In this case, as seen in **Figure 9**,
34 the presence of SAIL has no marked effect on the micelle size, with all solutions equilibrating to
35 a single large micellar aggregate. Furthermore, the PEG corona in L-31 is extremely small, which
36 means that even the phosphonium charged groups are rather exposed to the solution. Taken
37 together, this means that the L-31 system is the least sensitive to structural differences caused by
38 changing the head group type.
39
40
41
42
43
44
45

46 26 Changing the alkyl chain length of the imidazolium cations also has different effects depending
47 on the type of Pluronic system. For the smaller Pluronics, all the imidazolium cations induce nearly
48 the same increase in the cloud point, regardless of the chain length (at least for chains larger than
49 10 carbons). In contrast, for the larger Pluronics, [C₁₀mim]Cl has very little effect on the cloud
50 point temperature. Once again, this can be partly explained by the balance between hydrophobic
51 and electrostatic interactions in the mixed systems. For the small Pluronics, even the small
52
53
54
55
56
57
58
59
60

1
2
3 1 [C₁₀mim]Cl cation is able to accumulate at the surface and induce pronounced inter-micellar
4 2 repulsion. In the larger Pluronics, in particular for L-31, the smaller cation shows a much less
5 3 ordered arrangement at the surface, leading to weaker electrostatic repulsion. In addition, the
6 4 hydrophobic driving force for aggregation is much stronger, and effectively dominates the onset
7 5 of the cloud point.
8
9

10
11 We observed that at higher temperatures, the micelle PEG coronas are somewhat dehydrated,
12 6 which facilitates micelle fusion processes; However, this was not always the case Actually,
13 7 depending on the concentration, some Pluronic aqueous solutions can exhibit a weak temperature
14 8 impact in the micelle distribution⁵⁴ as also noticed by comparing the results shown in **Figures 2**
15 9 and **9**. **Table S5** displays the characteristics of the micelle distributions obtained in the MD
16 10 simulations at CPT for all systems. The L-31 and 31R1, both with relatively high PPG content,
17 11 showed a nearly temperature-independent micellar distribution. However, the 10R5 and L-35, with
18 12 similar PEG:PPG ratios, exhibited 3/4 micelles at 25°C, and 2/3 micelles at the CPT. Furthermore,
19 13 the addition of SAILs produced a different impact in the micelle distribution which also depends
20 14 on their nature, as discussed in more detail below. Additionally, all systems considered in this
21 15 work were run without Pluronics, *i.e.*, as SAIL aqueous solutions, and no more than one or two
22 16 SAIL micelles were found in all of the cases. Thus, it is clear that the interaction between Pluronic
23 17 and SAIL plays an important role affecting the micelle distribution in the mixed systems when
24 18 compared with their respective aqueous solutions.
25
26
27
28
29
30
31
32
33
34
35
36

37 20 It becomes clear from the micellar growth profiles shown in **Figure S4** and the final micellar
38 21 distribution displayed in **Table S5** that Pluronics become more thermo-responsive in the presence
39 22 of SAILs, except in the L-31 and 31R1 cases, where the relatively high PPG content dominates
40 23 the aggregation as it can be also noticed in the simulation snapshots displayed in **Figures 2** and **9**.
41 24 This fact was also confirmed in the CPT curves of L-31 and 31R1 obtained in the experiments
42 25 (**Figure 8**). The impact of SAILs observed in 10R5 and L-35, led us to conclude that the less
43 26 screened charge and more hydrophilic head-group of imidazolium in Pluronic micelles somehow
44 27 hinders the micelle growth.
45
46
47
48
49

50 28 **Table S5** also shows a diverse temperature effect depending on the Pluronic and SAIL nature.
51 29 Commonly, the temperature promotes micelle fusion processes increasing the sizes. In
52 30 Pluronic/[P_{4,4,4,14}]Cl mixtures at their CPTs (see **Table S2**), reverse Pluronics, 10R5/[P_{4,4,4,14}]Cl
53 31 (76°C) and 31R1/[P_{4,4,4,14}]Cl (27°C), showed bigger micelles but the size was practically unaffected
54
55
56
57
58
59
60

1
2
3 1 in normal Pluronics, L-35/[P_{4,4,4,14}]Cl (95°C) and L-31/[P_{4,4,4,14}]Cl (47°C). However, the
4 2 imidazolium exhibited a different behaviour with the 10R5/[C₁₄mim]Cl (88°C) displaying smaller
5 3 micelles whilst bigger ones were obtained in the L35/[C₁₄mim]Cl (95°C). Conversely, for low
6 4 PEG:PPG Pluronic ratios, the same number of micelles and N_a, were maintained, but the micelle
7 5 diameter was increased. **Table S6** shows a summary of the N_a and micelle diameter (\varnothing) evolution
8 6 when CPT is attained in each system.

9 7 The diverse trend exhibited above could be explained by the fact that the Pluronic/SAIL
10 8 micellar growth with temperature increase may depend on whether the SAIL presents an LCST or
11 9 UCST behaviour. Although the micelle size might not increase for an LCST system by fusion,
12 10 dehydration of the interface could allow for the formation of larger aggregates by coalescence.
13 11 This is similar to what we observed in our previous work with the [P_{4,4,4,14}]Cl system.⁵⁵ A
14 12 surfactant presenting an UCST behaviour, such as imidazolium ILs, can be considered more as a
15 13 traditional salt, for which we would expect a temperature increase to have less effect on the micelle
16 14 size. In addition, mixtures of Pluronic and SAILs are likely to exhibit an even more complex
17 15 behaviour compared with individual solutions of Pluronics and SAILs, and it is difficult to
18 16 extrapolate results based on a limited number of micelles to the complex phenomena of phase
19 17 separation.

20 18 Finally, it can be seen that the effect of SAIL on the cloud point is somewhat more pronounced
21 19 for the normal Pluronic L-35 than for the reverse Pluronic 10R5. Taking into account that both
22 20 polymers have the same composition, only differing in the arrangement of the PPG and PEG
23 21 blocks, suggests that the differences are purely related to surface effects. However, the effects of
24 22 the different SAIL cations on the micelle surface structure are also quite similar for these two
25 23 Pluronics (compare **Figures S8** and **S9**). The most probable explanation, therefore, lies in the
26 24 ability of 10R5 to form cross-links between micelles during self-assembly. As discussed in our
27 25 previous publication,⁷ this ability is responsible for the measured differences in the cloud points
28 26 of the two Pluronics in aqueous solutions without SAIL. When SAIL is added to the mixture, the
29 27 10R5 chains still retain their ability to cross-link in the very initial stages of the micelle formation
30 28 as shown in **Figure S11**. The initial cross-link aggregates, which only appear at the beginning, can
31 29 contribute to counteract the effect of electrostatic repulsion induced by the SAIL. This
32 30 circumstance facilitates the micelles to be closer to each other, despite the fact that in the final
33 31 equilibrium state, the micelles are separated. As a consequence, the SAIL effect is more

1 pronounced in the normal L-35 Pluronic, where cross-links are absent, and the system is dominated
2 by electrostatics.

4 **4. Conclusions**

5 This work provides a detailed study on the impact of SAILS on the cloud points of a series of
6 Pluronic copolymers with different characteristics, namely normal *vs* reverse, and with different
7 PEG content. In all cases, it was observed that the increase in the system hydrophobicity led to a
8 decrease in the cloud point temperature as a result of an intricate balance of hydrophobic forces
9 and inter micellar interactions. The more pronounced cloud point increase of the mixed
10 imidazolium-based systems was a result of the unscreened imidazolium charge in comparison with
11 the screened phosphonium head group. A weak alkyl-chain length effect was found in the micelle
12 distribution of mixtures of Pluronics with [C₁₀mim]Cl and [C₁₄mim]Cl. However, a more detailed
13 study including larger imidazolium and phosphonium alkyl-chain lengths is needed to shed further
14 light into this issue. The bulkier alkyl side chains of [P_{4,4,4,14}]Cl screen the SAIL charge and displace
15 it towards the inside of the Pluronic micelle core, reducing the impact of electrostatic repulsion
16 between neighbouring micelles and thus, favouring their coalescence. The chain length of the
17 imidazolium SAIL had virtually no effect on the cloud point of Pluronics with small cores and
18 large coronas, since even small cations were able to induce inter micellar repulsions. In contrast,
19 for Pluronics with larger cores, SAIL cations with larger chain lengths are needed to induce such
20 effects. Our results suggest that there may be a minimum cation chain length for each type of
21 Pluronic, below which the cloud point is not affected. More systematic studies on Pluronic/SAIL
22 mixtures with controlled sizes of hydrophobic groups are needed to confirm this assertion. The
23 overall impact of SAILS of the Pluronic micellar aqueous solutions addressed in this study was a
24 reduction in the micelle fusion events, increasing the number of aggregates compared with the
25 Pluronic aqueous solution references whilst the micelle size is increased by the presence of
26 adsorbed SAIL moieties. Although the measures described above give us confidence that the
27 results we are reporting correspond to thermodynamic equilibrium, we cannot exclude the
28 possibility of kinetic effects that are longer than the time scale of our simulations.

29 The remarkably simple and transferable model herein proposed herein was able to capture the
30 subtle differences in the behaviour of four distinct Pluronics in aqueous solution over a range of
31 concentrations from dilute to mildly concentrated⁷ as well as the interaction between dilute

1 solutions of SAILs and Pluronics. This represents a significant advancement in both simulation
2 and understanding of triblock copolymer aggregation. Experimental results, validated by the
3 simulations, indicate that the LCST transition for triblock copolymers can be varied by the careful
4 adjustment of the PEG:PPG ratio and the micelle surface characteristic, *i.e.* normal *vs* reverse
5 Pluronics, as previously reported.⁷ This can be further tuned by addition of small amounts of
6 SAILs. The nature of the SAIL and concentration as well as the SAIL-Pluronic interactions were
7 found to strongly influence the cloud point of the polymer. Ortona *et al.*²⁷ suggested that the
8 Pluronic-surfactant interactions are driven by a combination of several factors, in which some of
9 them can be distinct from the known surfactant-surfactant interactions. Surface functionalization
10 of the polymeric micelle by addition of an electrostatic component with different strength
11 (imidazolium *vs* phosphonium-based SAILs) is of significant interest for several fields. SAILs
12 were shown to extract a number of high value inorganic and organic compounds. This work offers
13 a predictive model to study different copolymers while elucidating the fundamental thermal
14 response of these systems, which is required for the cloud point extraction of distinct compounds.
15 Furthermore, this work provides, for the first time, an intuitive computer simulation framework to
16 study mixtures of Pluronics and SAILs, opening the door for designing tailor-made thermal
17 controlled solvents by computer simulations.

Supporting Information

The Supporting Information is available free of charge on the ACS Publications website at DOI:XXX.

Characteristics of the Pluronic systems used in this study, the PPG and PEG content, % in PEG and molecular weight as well as a description of all simulation runs carried out at 25°C and CPT. Experimental binodal CPT curves for all Pluronic aqueous solutions and the SAIL mixtures up to 18 wt% of Pluronic concentration. Detailed description of the initial stages of micelle formation of L-35 and L-31 and their mixtures with [C₁₄mim]Cl and [P_{4,4,4,14}]Cl at 25°C. A detailed picture of the initial stages of L-35 with [C₁₄mim]Cl and [P_{4,4,4,14}]Cl mixtures at 25°C with 0.3 wt% of SAIL concentration where L-35, SAIL monomers and hybrid L-35/SAIL aggregates are shown. Micelle density profiles of 10R5, L-35 and 31R1 aqueous solutions and after addition of [C₁₀mim]Cl, [C₁₄mim]Cl and [P_{4,4,4,14}]Cl. A detailed picture of the initial stages of the 10R5 + [C₁₄mim]Cl micelle formation at the CPT highlighting cross-linked formation.

Acknowledgements

This work was developed within the scope of the project CICECO-Aveiro Institute of Materials, UIDB/50011/2020 & UIDP/50011/2020, financed by national funds through the FCT/MEC and when appropriate co-financed by FEDER under the PT2020 Partnership Agreement. The authors are also grateful for the national fund through the Portuguese Foundation for Science and Technology (FCT) for the doctoral grant SFRH/BD/101683/2014 of F.A. Vicente. German Perez-Sanchez and Nicolas Schaeffer acknowledge the national funds (OE), through FCT – Fundação para a Ciência e a Tecnologia, I.P., in the scope of the framework contract foreseen in the numbers 4, 5 and 6 of the article 23, of the Decree-Law 57/2016, of August 29, changed by Law 57/2017, of July 19.

References

- (1) Bodratti, A.; Alexandridis, P. Formulation of Poloxamers for Drug Delivery. *J. Funct. Biomater.* **2018**, *9* (1), 11.
- (2) Wang, Y.; Hu, X.; Han, J.; Ni, L.; Tang, X.; Hu, Y.; Chen, T. Integrated Method of Thermosensitive Triblock Copolymer–Salt Aqueous Two Phase Extraction and Dialysis Membrane Separation for Purification of Lycium Barbarum Polysaccharide. *Food Chem.* **2016**, *194*, 257–264.
- (3) de Lemos, L. R.; Campos, R. A.; Rodrigues, G. D.; da Silva, L. H. M.; da Silva, M. C. H. Green Separation of Copper and Zinc Using Triblock Copolymer Aqueous Two-Phase Systems. *Sep. Purif. Technol.* **2013**, *115*, 107–113.
- (4) Wanka, G.; Hoffmann, H.; Ulbricht, W. Phase Diagrams and Aggregation Behavior of Poly (Oxyethylene)-Poly (Oxypropylene)-Poly (Oxyethylene) Triblock Copolymers in Aqueous Solutions. *Macromolecules* **1994**, *27* (15), 4145–4159.
- (5) Mortensen, K.; Brown, W.; Joergensen, E. Phase Behavior of Poly(Propylene Oxide)-Poly(Ethylene Oxide)-Poly(Propylene Oxide) Triblock Copolymer Melt and Aqueous Solutions. *Macromolecules* **1994**, *27* (20), 5654–5666.
- (6) Tsui, H.-W.; Wang, J.-H.; Hsu, Y.-H.; Chen, L.-J. Study of Heat of Micellization and Phase Separation for Pluronic Aqueous Solutions by Using a High Sensitivity Differential Scanning Calorimetry. *Colloid Polym. Sci.* **2010**, *288* (18), 1687–1696.
- (7) Pérez-Sánchez, G.; Vicente, F. A.; Schaeffer, N.; Cardoso, I. S.; Ventura, S. P. M.; Jorge, M.; Coutinho, J. A. P. Rationalizing the Phase Behavior of Triblock Copolymers through Experiments and Molecular Simulations. *J. Phys. Chem. C* **2019**, *123* (34), 21224–21236.
- (8) Soares, R. R. G.; Azevedo, A. M.; Van Alstine, J. M.; Aires-Barros, M. R. Partitioning in Aqueous Two-Phase Systems: Analysis of Strengths, Weaknesses, Opportunities and Threats. *Biotechnol. J.* **2015**, *10* (8), 1158–1169.
- (9) Blesic, M.; Marques, M. H.; Plechkova, N. V.; Seddon, K. R.; Rebelo, L. P. N.; Lopes, A. Self-Aggregation of Ionic Liquids: Micelle Formation in Aqueous Solution. *Green Chem.*

- 1
2
3 1 **2007**, 9 (5), 481–490.
4
5
6 2 (10) Dong, B.; Li, N.; Zheng, L.; Yu, L.; Inoue, T. Surface Adsorption and Micelle Formation
7 3 of Surface Active Ionic Liquids in Aqueous Solution. *Langmuir* **2007**, 23 (8), 4178–4182.
8
9
10 4 (11) Smirnova, N. a; Vanin, A. a; Safonova, E. a; Pukinsky, I. B.; Anufrikov, Y. a; Makarov, A.
11 5 L. Self-Assembly in Aqueous Solutions of Imidazolium Ionic Liquids and Their Mixtures
12 6 with an Anionic Surfactant. *J. Colloid Interface Sci.* **2009**, 336 (2), 793–802.
13
14
15
16 7 (12) Singh, D. K.; Sastry, N. V; Trivedi, P. A. Amphiphilic Copolymers and Surface Active
17 8 Ionic Liquid Systems in Aqueous Media – Surface Active and Aggregation Characteristics.
18 9 *Colloids Surfaces A Physicochem. Eng. Asp.* **2017**, 524, 111–126.
19
20
21
22 10 (13) Behera, K.; Pandey, S. Interaction between Ionic Liquid and Zwitterionic Surfactant: A
23 11 Comparative Study of Two Ionic Liquids with Different Anions. *J. Colloid Interface Sci.*
24 12 **2009**, 331 (1), 196–205.
25
26
27
28 13 (14) Singh, K.; Marangoni, D. G.; Quinn, J. G.; Singer, R. D. Spontaneous Vesicle Formation
29 14 with an Ionic Liquid Amphiphile. *J. Colloid Interface Sci.* **2009**, 335 (1), 105–111.
30
31
32
33 15 (15) Pramanik, R.; Sarkar, S.; Ghatak, C.; Rao, V. G.; Mandal, S.; Sarkar, N. Effects of 1-Butyl-
34 16 3-Methyl Imidazolium Tetrafluoroborate Ionic Liquid on Triton X-100 Aqueous Micelles:
35 17 Solvent and Rotational Relaxation Studies. *J. Phys. Chem. B* **2011**, 115 (21), 6957–6963.
36
37
38
39 18 (16) Chen, L. G.; Bermudez, H. Solubility and Aggregation of Charged Surfactants in Ionic
40 19 Liquids. *Langmuir* **2012**, 28 (2), 1157–1162.
41
42
43 20 (17) Chen, L. G.; Bermudez, H. Charge Screening between Anionic and Cationic Surfactants in
44 21 Ionic Liquids. *Langmuir* **2013**, 29 (9), 2805–2808.
45
46
47 22 (18) Miskolczy, Z.; Sebők-Nagy, K.; Biczók, L.; Göktürk, S. Aggregation and Micelle
48 23 Formation of Ionic Liquids in Aqueous Solution. *Chem. Phys. Lett.* **2004**, 400 (4–6), 296–
49 24 300.
50
51
52
53 25 (19) Umapathi, R.; Venkatesu, P. Thermo-Responsive Triblock Copolymer Phase Transition
54 26 Behaviour in Imidazolium-Based Ionic Liquids: Role of the Effect of Alkyl Chain Length

- 1
2
3 1 of Cations. *J. Colloid Interface Sci.* **2017**, *485*, 183–191.
4
5
6 2 (20) Madhusudhana Reddy, P.; Venkatesu, P. Influence of Ionic Liquids on the Critical
7 3 Micellization Temperature of a Tri-Block Co-Polymer in Aqueous Media. *J. Colloid*
8 4 *Interface Sci.* **2014**, *420*, 166–173.
9
10
11 5 (21) Lunagariya, J.; Kumar, N. S.; Asif, M.; Dhar, A.; Vekariya, R. L. Dependency of Anion and
12 6 Chain Length of Imidazolium Based Ionic Liquid on Micellization of the Block Copolymer
13 7 F127 in Aqueous Solution: An Experimental Deep Insight. *Polymers (Basel)*. **2017**, *9* (7),
14 8 285.
15
16
17 9 (22) Khan, I.; Umapathi, R.; Neves, M. C.; Coutinho, J. A. P.; Venkatesu, P. Structural Insights
18 10 into the Effect of Cholinium-Based Ionic Liquids on the Critical Micellization Temperature
19 11 of Aqueous Triblock Copolymers. *Phys. Chem. Chem. Phys.* **2016**, *18* (12), 8342–8351.
20
21
22 12 (23) Phani Kumar, B. V. N.; Reddy, R. R.; Pan, A.; Aswal, V. K.; Tsuchiya, K.; Prameela, G.
23 13 K. S.; Abe, M.; Mandal, A. B.; Moulik, S. P. Physicochemical Understanding of Self-
24 14 Aggregation and Microstructure of a Surface-Active Ionic Liquid [C4mim] [C8OSO3]
25 15 Mixed with a Reverse Pluronic 10R5 (PO8EO22PO8). *ACS Omega* **2018**, *3* (5), 5155–5164.
26
27
28 16 (24) Zheng, L.; Guo, C.; Wang, J.; Liang, X.; Chen, S.; Ma, J.; Yang, B.; Jiang, Y.; Liu, H. Effect
29 17 of Ionic Liquids on the Aggregation Behavior of PEO-PPO-PEO Block Copolymers in
30 18 Aqueous Solution. *J. Phys. Chem. B* **2007**, *111* (6), 1327–1333.
31
32
33 19 (25) Dai, S.; Tam, K. C.; Li, L. Isothermal Titration Calorimetric Studies on Interactions of Ionic
34 20 Surfactant and Poly(Oxypropylene)–Poly(Oxyethylene)– Poly(Oxypropylene) Triblock
35 21 Copolymers in Aqueous Solutions. *Macromolecules* **2001**, *34* (20), 7049–7055.
36
37
38 22 (26) Mata, J.; Joshi, T.; Varade, D.; Ghosh, G.; Bahadur, P. Aggregation Behavior of a PEO–
39 23 PPO–PEO Block Copolymer + Ionic Surfactants Mixed Systems in Water and Aqueous Salt
40 24 Solutions. *Colloids Surfaces A Physicochem. Eng. Asp.* **2004**, *247* (1–3), 1–7.
41
42
43 25 (27) Ortona, O.; D’Errico, G.; Paduano, L.; Vitagliano, V. Interaction between Cationic,
44 26 Anionic, and Non-Ionic Surfactants with ABA Block Copolymer Pluronic PE6200 and with
45 27 BAB Reverse Block Copolymer Pluronic 25R4. *J. Colloid Interface Sci.* **2006**, *301* (1), 63–
46
47
48
49
50
51
52
53
54
55
56
57
58
59
60

- 1
2
3 1 77.
4
5
6 2 (28) Sharma, R.; Kang, T. S.; Mahajan, R. K. Complexation of Triblock Reverse Copolymer
7 3 10R5 with Surface Active Ionic Liquids in Aqueous Medium: A Physico-Chemical Study.
8 4 *RSC Adv.* **2015**, 5 (21), 16349–16360.
9
10
11 5 (29) Liu, X.; Hu, J.; Huang, Y.; Fang, Y. Aggregation Behavior of Surface Active
12 6 Dialkylimidazolium Ionic Liquids [C₁₂C_nim]Br (n =1–4) in Aqueous Solutions. *J.*
13 7 *Surfactants Deterg.* **2013**, 16 (4), 539–546.
14
15
16 8 (30) Vicente, F. A.; Malpiedi, L. P.; Silva, F. A. e; Jr., A. P.; Coutinho, J. A. P.; Ventura, S. P.
17 9 M. Design of Novel Aqueous Micellar Two-Phase Systems Using Ionic Liquids as Co-
18 10 Surfactants for the Selective Extraction of (Bio)Molecules. *Sep. Purif. Technol.* **2014**, 135,
19 11 259–267.
20
21
22 12 (31) Vicente, F. A.; Cardoso, I. S.; Sintra, T. E.; Lemus, J.; Marques, E. F.; Ventura, S. P. M.;
23 13 Coutinho, J. A. P. Impact of Surface Active Ionic Liquids on the Cloud Points of Nonionic
24 14 Surfactants and the Formation of Aqueous Micellar Two-Phase Systems. *J. Phys. Chem. B*
25 15 **2017**, 121 (37), 8742–8755.
26
27
28 16 (32) Schaeffer, N.; Passos, H.; Gras, M.; Mogilireddy, V.; Leal, J. P.; Perez-Sanchez, G.; Gomes,
29 17 J. R. B.; Billard, I.; Papaiconomou, N.; Coutinho, J. A. P. Mechanism of Ionic-Liquid-Based
30 18 Acidic Aqueous Biphasic System Formation. *Phys. Chem. Chem. Phys.* **2018**.
31
32
33 19 (33) Crespo, E. A.; Schaeffer, N.; Coutinho, J. A. P.; Perez-Sanchez, G. Improved Coarse-Grain
34 20 Model to Unravel the Phase Behavior of 1-Alkyl-3-Methylimidazolium-Based Ionic
35 21 Liquids through Molecular Dynamics Simulations. *J. Colloid Interface Sci.* **2020**, 574, 324–
36 22 336.
37
38
39 23 (34) Marrink, S. J.; Risselada, H. J.; Yefimov, S.; Tieleman, D. P.; de Vries, A. H. The MARTINI
40 24 Force Field: Coarse Grained Model for Biomolecular Simulations. *J. Phys. Chem. B* **2007**,
41 25 111 (27), 7812–7824.
42
43
44 26 (35) Alessandri, R.; Uusitalo, J. J.; De Vries, A. H.; Havenith, R. W. A.; Marrink, S. J. Bulk
45 27 Heterojunction Morphologies with Atomistic Resolution from Coarse-Grain Solvent
46
47
48
49
50
51
52
53
54
55
56
57
58
59
60

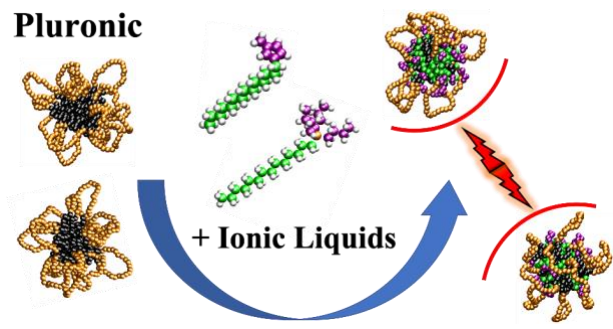
- 1
2
3 1 Evaporation Simulations. *J. Am. Chem. Soc.* **2017**, *139* (10), 3697–3705.
4
5
6 2 (36) Vazquez-Salazar, L. I.; Selle, M.; de Vries, A. H.; Marrink, S.-J.; Souza, P. C. T. Martini
7 3 Coarse-Grained Models of Imidazolium-Based Ionic Liquids: From Nanostructural
8 4 Organization to Liquid-Liquid Extraction. **2020**.
9
10
11 5 (37) Panizon, E.; Bochicchio, D.; Monticelli, L.; Rossi, G. MARTINI Coarse-Grained Models
12 6 of Polyethylene and Polypropylene. *J. Phys. Chem. B* **2015**, *119* (25), 8209–8216.
13
14
15
16 7 (38) Abraham, M. J.; Murtola, T.; Schulz, R.; Páll, S.; Smith, J. C.; Hess, B.; Lindahl, E.
17 8 GROMACS: High Performance Molecular Simulations through Multi-Level Parallelism
18 9 from Laptops to Supercomputers. *SoftwareX* **2015**, *1–2*, 19–25.
19
20
21
22 10 (39) Hockney, R. .; Goel, S. .; Eastwood, J. . Quiet High-Resolution Computer Models of a
23 11 Plasma. *J. Comput. Phys.* **1974**, *14* (2), 148–158.
24
25
26
27 12 (40) Verlet, L. Computer “Experiments” on Classical Fluids. I. Thermodynamical Properties of
28 13 Lennard-Jones Molecules. *Phys. Rev.* **1967**, *159* (1), 98–103.
29
30
31 14 (41) Darden, T.; York, D.; Pedersen, L. Particle Mesh Ewald: An $N \cdot \log(N)$ Method for Ewald
32 15 Sums in Large Systems. *J. Chem. Phys.* **1993**, *98* (12), 10089–10092.
33
34
35 16 (42) Hess, B.; Bekker, H.; Berendsen, H. J. C.; Fraaije, J. G. E. M. LINCS: A Linear Constraint
36 17 Solver for Molecular Simulations. *J. Comput. Chem.* **1997**, *18* (12), 1463–1472.
37
38
39 18 (43) Bussi, G.; Donadio, D.; Parrinello, M. Canonical Sampling through Velocity Rescaling. *J.*
40 19 *Chem. Phys.* **2007**, *126* (1), 014101.
41
42
43 20 (44) Hoover, W. G. Canonical Dynamics: Equilibrium Phase-Space Distributions. *Phys. Rev. A*
44 21 **1985**, *31* (3), 1695–1697.
45
46
47
48 22 (45) Nosé, S. A Unified Formulation of the Constant Temperature Molecular Dynamics
49 23 Methods. *J. Chem. Phys.* **1984**, *81* (1), 511–519.
50
51
52 24 (46) Parrinello, M.; Rahman, A. Polymorphic Transitions in Single Crystals: A New Molecular
53 25 Dynamics Method. *J. Appl. Phys.* **1981**, *52* (12), 7182–7190.
54
55
56
57
58
59
60

- 1
2
3 1 (47) Humphrey, W.; Dalke, A.; Schulten, K. VMD: Visual Molecular Dynamics. *J. Mol. Graph.*
4 **1996**, *14* (1), 33–38.
5 2
6
7 3 (48) Jorge, M. Molecular Dynamics Simulation of Self-Assembly of n -
8 Decyltrimethylammonium Bromide Micelles. *Langmuir* **2008**, *24* (11), 5714–5725.
9 4
10
11 5 (49) Pérez-Sánchez, G.; Gomes, J. R. B.; Jorge, M. Modeling Self-Assembly of Silica/Surfactant
12 Mesostructures in the Templated Synthesis of Nanoporous Solids. *Langmuir* **2013**, *29* (7).
13 6
14
15 7 (50) Hoshen, J.; Kopelman, R. Percolation and Cluster Distribution. I. Cluster Multiple Labeling
16 Technique and Critical Concentration Algorithm. *Phys. Rev. B* **1976**, *14* (8), 3438–3445.
17 8
18
19 9 (51) Pérez-Sánchez, G.; Vicente, F. A.; Schaeffer, N.; Cardoso, I. S.; Ventura, S. P. M.; Jorge,
20 M.; Coutinho, J. A. P. Rationalizing the Phase Behavior of Triblock Copolymers through
21 Experiments and Molecular Simulations. *J. Phys. Chem. C* **2019**, *123* (34), 21224–21236.
22 10
23
24 11 (52) Blesic, M.; Marques, M. H.; Plechkova, N. V.; Seddon, K. R.; Rebelo, L. P. N.; Lopes, A.
25 Self-Aggregation of Ionic Liquids: Micelle Formation in Aqueous Solution. *Green Chem.*
26 **2007**, *9* (5), 481–490.
27 12
28
29 13 (53) Torres, F. A. E.; de Almeida Francisco, A. C.; Pereira, J. F. B.; Santos-Ebinuma, V. de C.
30 Imidazolium-Based Ionic Liquids as Co-Surfactants in Aqueous Micellar Two-Phase
31 Systems Composed of Nonionic Surfactants and Their Aptitude for Recovery of Natural
32 Colorants from Fermented Broth. *Sep. Purif. Technol.* **2018**, *196*, 262–269.
33 15
34
35 16 (54) Alexandridis, P.; Alan Hatton, T. Poly(Ethylene Oxide)□poly(Propylene
36 Oxide)□poly(Ethylene Oxide) Block Copolymer Surfactants in Aqueous Solutions and at
37 Interfaces: Thermodynamics, Structure, Dynamics, and Modeling. *Colloids Surfaces A*
38 *Physicochem. Eng. Asp.* **1995**, *96* (1–2), 1–46.
39 22
40
41 19 (55) Schaeffer, N.; Pérez-Sánchez, G.; Passos, H.; Gomes, J. R. B.; Papaiconomou, N.;
42 Coutinho, J. A. P. Mechanisms of Phase Separation in Temperature-Responsive Acidic
43 Aqueous Biphasic Systems. *Phys. Chem. Chem. Phys.* **2019**, *21* (14), 7462–7473.
44 21
45
46 22
47
48 23
49 24
50 25
51
52
53
54 26
55
56
57
58
59
60

1
2
3
4
5
6
7
8
9
10
11
12
13
14
15
16
17
18
19
20
21
22
23
24
25
26
27
28
29
30
31
32
33
34
35
36
37
38
39
40
41
42
43
44
45
46
47
48
49
50
51
52
53
54
55
56
57
58
59
60

1

TOC Graphic



2